Bladder tissue biomechanical behavior: experimental tests and constitutive formulation

A.N. Natali[a,b,] A.L. Audenino[c], W. Artibani[d], C.G. Fontanella[a,*], E.L. Carniel[a,b], E.M. Zanetti[e]

[a] Centre for Mechanics of Biological Materials, University of Padova, Via F. Marzolo 9, I - 35131 Padova, Italy

[b] Department of Industrial Engineering, University of Padova, Via F. Marzolo 9, I - 35131 Padova, Italy

[c] Department of Mechanical and Aerospatial Engineering, Politecnico di Torino, Corso Duca degli Abruzzi 24 - 10129 Torino, Italy

[d] University of Verona, Department of Urology, Policlinico G.B. Rossi, Ospedale Borgo Roma, P.le L.A. Scuro 10, 37134, Verona, Italy

[e] Department of Engineering, University of Perugia, Via Duranti 65 - 06125, Perugia, Italy

***Corresponding author**

Arturo N Natali

Centre for Mechanics of Biological Materials

University of Padova,

Via F. Marzolo 9, I-35131 Padova (ITALY)

Tel. +39 (0)49 827 5598 – Fax +39 (0)49 827 5604

E-mail: arturo.natali@unipd.it

ABSTRACT

A procedure for the constitutive analysis of bladder tissues mechanical behavior is provided, by using a coupled experimental and computational approach. The first step pertains to the design and development of mechanical tests on specimens from porcine bladders. The bladders have been harvested, and the specimens have been subjected to uniaxial cyclic tests at different strain rates along preferential directions, considering the distribution of tissue fibrous components. Experimental results showed the anisotropic, non-linear and time-dependent stress-strain behavior, due to tissue conformation with fibers distributed along preferential directions and their interaction phenomena with ground substance. In detail, experimental data showed a greater tissue stiffness along transversal direction. Viscous behavior was assessed by strain rate dependence of stress-strain curves and hysteretic phenomena. The second step pertains the development of a specific fiber-reinforced visco-hyperelastic constitutive model, in the light of bladder tissues structural conformation and experimental results. Constitutive parameters have been identified by minimizing the discrepancy between model and experimental data. The agreement between experimental and model results represent a term for evaluating the reliability of the constitutive models by means of the proposed operational procedure.

KEYWORDS:

Bladder, soft tissue mechanics, experimental test, non-linear mechanics, computational approach.

Bladder tissue biomechanical behavior: experimental tests and constitutive formulation

INTRODUCTION

Lower urinary tract dysfunction affects about 400 million people worldwide because of mechanical, neurological or idiopathic insult. Different congenital or acquired pathologies determine anatomical and functional alterations also of the bladder-sphinteric apparatus with consequent impaired urinary continence (Korossis et al., 2009, Irwin et al., 2006, Sacco et al., 2006). An engineering approach can provide reliable tools for the treatments of pathologic situations, as to design the most appropriate long-term surgical repair procedures or to investigate and develop materials for bladder reconstruction.

The structural models of specific organs is addressed, by a computational approach, to the investigation of the mechanical response of biological tissue and structures in health and disease, also to analyze interaction phenomena with biomedical devices (Carniel et al., 2013; Carniel et al., 2014; Krywonos et al., 2010). The definition of computational models requires both 3D virtual solid models of anatomical region and reliable constitutive formulations of biological tissues. As matter of example, the three dimensional reconstruction of the pelvic district, as virtual solid models, by reverse engineering techniques has proved to be useful for preoperative planning, allowing to analyze the outcomes of different reconstructive solutions or to support diagnostic hypotheses (Chai et al., 2012; Hampel et al, 2004; Marino and Bignardi, 2002; Pel and van Mastrigt, 2007; Vlastelica et al., 2007). The constitutive analysis of soft biological tissues mechanics is usually performed by a coupled experimental and computational approach. Mechanical tests must be accurately designed accounting for the expected tissue properties, considering anisotropic behavior, non-linear effects and time-dependent phenomena, evaluating the tissue structural configuration. The experimental results allows to provide the appropriate constitutive formulation and to identify the associated parameters.

Different authors reported investigations about bladder tissues mechanics, with regard to both experimental and computational activities. Regnier et al. (1983) provided hyperelastic formulation to interpret the non-linear elastic behavior. Salinas et al. (1992) and Nagatomi et al. (2004) developed experimental activities to evaluate the viscoelastic properties together with preliminary model formulation. Van Mastrigt et al (1981) carried out an investigation of the strain rate dependence of the viscoelastic response of the urinary bladder wall. Korossis et al. (2009) and Chen et al. (2013) investigated the anisotropic and non-linear elastic behavior by experimental activities, considering also the relationship between the tissue histo-architecture and mechanical properties.

The improvement provided by the current study is the combined action of experimental and numerical approach for the analysis of the bladder tissue mechanics, aiming at a reciprocal reliability assessment. Specific experimental tests are developed and, considering histological configuration and experimental results, an appropriate constitutive model is implemented.

Some general notes are reported with regard to the histomorphometric configuration of the bladder tissue, aiming at the biomechanical characterization. The wall is a complex structure made up of mucosa, submucosa, muscolaris and serosa layers as reported by different authors (Bouhout et al., 2013; Zanetti et al., 2012). The mucosa is the innermost tissue and consists of transitional epithelial cells layers, which adapt their shape to the bladder filling. The submucosa is a thick layer of loose connective tissue and it is rich in elastic fibers, nerve, blood and lymphatic vessels. The tunica muscolaris is composed of three smooth muscular layers together with connective elements. Within the inner and the outer layers, muscular fibers are predominately distributed from the apex to the bottom of the bladder, while a circumferential organization characterizes the fibers within the middle layer. The serosa layer is a visceral peritoneum and the mechanical contribution to the wall stiffness and strength in almost negligible. With regard to the overall contribution of connective fibers, elastin provides the recoiling mechanism of the tissues (Korossis et al. 2009), while collagen fibers are preferentially aligned along apex to base direction (Gilbert et al., 2009).

Such a complex configuration, with particular regard to fibrous components, entails the anisotropic and non-linear behavior. Fibrous structures, as muscular and connective ones, undergo stiffening phenomena with stretch, leading to non-linear elastic properties. Micro-structural rearrangement phenomena, as fibers uncrimping and interaction with liquid components, lead to viscous effects (Bouhout et al., 2013; Korossis et al. 2009; Zanetti et al., 2012). Aiming at the mechanical characterization, tensile tests on tissue specimens are developed along different directions and at different strain rates. A constitutive formulations is developed in the framework of a theory that accounts for anisotropic behavior, coupled geometrical and material non-linearity and time-dependent phenomena. The identification of constitutive parameters is performed comparing model results and data from mechanical tests by fitting procedures. The reliability of constitutive formulation and parameters obtained is assessed by comparison of computational and experimental results with reference to additional experimental tests.

MATERIALS AND METHODS

Mechanical tests

The experimental tests have been performed on tissue specimens from pig bladder, because of the extensively supported similarity of pig and human tissues mechanics. Different authors (Dahms et al. 1998; Korossis et al. 2009) investigated bladder of different species, finding that pig and human bladder tissues show similar histomorphometric conformation and mechanical behavior. The intact bladders of three Large White pigs, that were 11-13 months old and about 160 Kg in weight, were collected from a local abattoir and transferred to the laboratory. The bladders were cleaned for luminal contents, adjacent tissues were dissected and the organs were frozen at -20°C. Twenty-four hours before testing, bladders were put into the fridge and completely defrosted (Dahms et al. 1998). They were dissected along the apex-to-base line, and samples were harvested from the lateral region of the wall. In detail, specimens were isolated using an I-shaped die cutter along apex-to-base (AB) direction and along transverse (T) direction (Figure 1). This shape prevented sample from over-stressing next to the grips, as witnessed by frequent failure in this area in the case of constant section specimens. Specimens were measured by means of photogrammetry to identify the central region and to evaluate width and thickness profiles using the image analysis software ImageJ (Zanetti et al. 2012). The number of specimens and their average width and thickness are reported in Table 1, while the length of each specimen in the central region of the I-shape was 12 mm. The length of the specimen has been chosen in relation to the limits of the loading machine and in agreement with the efficacy of the experimental tests performed (Bose Electroforce® 3200; 225 N maximum force; 12 mm stroke; static to 300 Hz frequency response), considering a 100% strain was to be reached. After their isolation, specimens were stored in the fridge within glass tubes containing PBS for less than 10 h. During tests, samples were continuously dampened with the solution to keep them wet.

A Bose Electroforce® equipment was used to perform tensile tests on the tissue specimens. Because of preliminary evaluation of samples strength, a load cell with capacity of 200 N with accuracy of ±0.1% was adopted. Clamping of the specimens was performed by grips (5 mm length and 20 mm wide), according to an intensity of about 100 kPa, adjusted to avoid the slippage and the damage of the specimens. The slippage has been checked during tests looking at the overall trend in the force/displacement curve. At the end of tests, it was verified that the length of the specimen clamped remained unchanged, and that there were no marks of longitudinal slips.Force and displacement signals were synchronized by means of a trigger signal. The displacement sensor measured clamp-to-clamp displacement while the load cell was placed below the specimen in correspondence of the fixed end. The reference point for zero-displacement was obtained applying a force threshold equal to 0.1 N (Mavrilas et al., 2005). The test protocol accounted for a first test of stress relaxation followed by cyclic tests at different strain rates. The stress relaxation test was performed reaching a grip displacement of 12 mm (corresponding to an axial strain of 100%) with a strain rate of 1.33%/s, followed by a 600 s holding time.

Subsequently, cyclic tests were performed reaching a strain of about 50%. Loading and unloading steps were performed accounting for different strain rates, as 10, 50, 100, 200, 500 %/s. The specific strain rates were defined considering results from constitutive investigations developed by other authors (Van Mastrigt et al., 1981; Salinas et al., 1992; Nagatomi et al., 2004). High strain rates, even overcoming physiological limits, support the overall analysis with regard to the constitutive formulation. In detail, such analyses led to relaxation times ranging between 10^{-1} and 10^{1} seconds and testing times were consequently defined.

During tests, load and displacement were acquired from a load cell and a linear differential transformer, respectively. The signals were acquired at 2 kHz sampling frequency.

Accounting for the undeformed geometrical conformation of the experimental specimens, load versus displacement data were converted to nominal stress versus stretch data. The stress was defined according to the Lagrangian scheme as the ratio of load to unload cross-sectional area, whereas the axial strain was defined as displacement refereed to the initial specimen length that is the distance between fixtures (Dahms et al. 1998). Results from cyclic tests on tissue specimens were post-processed to identify average nominal stress-stretch curves and scatter bands.

Constitutive formulation

Conformation of bladder wall must be investigate to interpret the overall mechanical behavior. It must be pointed out, for example, that fact that submucosa and muscular layers mainly contribute to the wall stiffness and strength. Such layers are composed of fibrous structures, as collagen and elastin in submucosa and smooth muscular fibers in muscular layers, embedded within an isotropic ground matrix. With particular regard to muscular layers, fibers are locally distributed along two main preferential directions determining the anisotropic behavior. The conformation of fibers and the interaction phenomena with ground substance entail non-linear elasticity and time dependent phenomena (Natali et al. 2004). A visco-hyperelastic constitutive formulation is assumed to interpret the typical features of the tissue mechanical response. The model accounts for the following Helmholtz free energy function (Natali et al. 2010, 2011):

$$\psi\left(\mathbf{C},\mathbf{q}^{i}\right)=W^{0}\left(\mathbf{C}\right)-\sum_{i=1}^{n}\int_{0}^{t}\frac{1}{2}\,\mathbf{q}^{i}:\dot{\mathbf{C}}\,dt \qquad (1)$$

where W^{0} is an hyperelastic potential that specifies the instantaneous response of the tissue, while $\mathbf{C}$ is the right Cauchy-Green strain tensor. Viscous variables $\mathbf{q}^{i}$ quantify the relaxation of stress components during loading. Structural rearrangement mechanisms of tissue elements over time entail such relaxation phenomena.

The specific hyperelastic potential is defined accounting for formulations that already proved their reliability in the framework of soft tissues mechanics (Fontanella et al., 2012; Fontanella et al., 2013; Forestiero et al., 2014), recalling that the mechanical behavior is determined by the properties of ground matrix and fibers and, consequently, the strain energy function can be additively decomposed:

$$W^0(\mathbf{C}) = W_m^0(\mathbf{C}) + W_f{}^0(\mathbf{C}, \mathbf{a}_0, \mathbf{b}_0) \tag{2}$$

where W_m and W_f refer to the ground matrix and fibers contributions, respectively, while $\mathbf{a}_0$ and $\mathbf{b}_0$ provide the preferential directions of fibrous elements, along apex-to-base and transverse directions, respectively.

The high liquid content of ground matrix determines the typical almost incompressible behavior of soft biological tissues (Weiss et al., 1996), and the following formulation of the ground matrix hyperelastic term W_m^0 is proposed (Natali et al., 2012):

$$W_m^0(\mathbf{C}) = -p(I_3 - 1) + \tilde{W}_m^0(\tilde{I}_1) \tag{3}$$

$$\tilde{W}_m^0(\tilde{I}_1) = [C_1/\alpha_1]\left\{\exp\left[\alpha_1(\tilde{I}_1 - 3)\right] - 1\right\} \tag{4}$$

where $\tilde{I}_1$ is the first iso-volumetric invariant of the right Cauchy-Green strain tensor, as $\tilde{I}_1 = \mathrm{tr}\left(I_3{}^{-1/3}\mathbf{C}\right)$, and I_3 is the third invariant, as $I_3 = \det(\mathbf{C})$. The term p serves as a Lagrange multiplier to ensure the kinematic constraint of almost incompressible continuum. Constitutive parameter C_1 specifies the tissue shear stiffness as $G = 2C_1$, while parameter α_1 regulates the non-linearity of the shear response, with reference to experimental results.

The definition of fibers contribution has to account for fibers rearrangement phenomena with stretch. A specific exponential formulation is provided (Natali et al., 2012):

$$W_f^{\,0}\left(\mathbf{C},\mathbf{a}_0,\mathbf{b}_0\right)=W_{fAB}\left(I_4\right)+W_{fT}\left(I_6\right) \tag{5}$$

$$W_{fAB}^0\left(I_4\right)=\left[C_4/\alpha_4^{\,2}\right]\left\{\exp\left[\alpha_4\left(I_4-1\right)\right]-\alpha_4\left(I_4-1\right)-1\right\} \tag{6}$$

$$W_{fT}^0\left(I_6\right)=\left[C_6/\alpha_6^{\,2}\right]\left\{\exp\left[\alpha_6\left(I_6-1\right)\right]-\alpha_6\left(I_6-1\right)-1\right\} \tag{7}$$

where I_4 and I_6 are structural invariants that specify tissue stretch along directions $\mathbf{a}_0$ and $\mathbf{b}_0$, respectively. The constitutive parameters C_4 and C_6 are constants that define the fibers initial stiffness, while α_4 and α_6 depend on fibers stiffening with stretch. Once the hyperelastic potentials have been specified, the stress-strain relationship can be computed accounting for thermo-mechanics principles (Natali et al., 2010):

$$\mathbf{P}\left(\mathbf{C},\mathbf{q}^i\right)=2\mathbf{F}\frac{\partial\psi\left(\mathbf{C},\mathbf{q}^i\right)}{\partial\mathbf{C}}=\mathbf{P}^0\left(\mathbf{C}\right)-\sum_{i=1}^{n}\mathbf{q}^i \tag{8}$$

$$\mathbf{P}^0\left(\mathbf{C}\right)=2\mathbf{F}\frac{\partial W^0\left(\mathbf{C}\right)}{\partial\mathbf{C}} \tag{9}$$

where $\mathbf{P}$ is the first Piola-Kirchhoff stress tensor and $\mathbf{F}$ is the deformation gradient. Accounting for the proposed formulation of the strain energy function, the nominal stress tensor contributions from the ground matrix and fibers families are defined as it follows:

$$\mathbf{P}_m^0=2\mathbf{F}\,\partial W_m/\partial\mathbf{C}=-p\mathbf{F}^{-T}+C_1\exp\left[\alpha_1\left(\tilde{I}_1-3\right)\right]\left(2J^{-2/3}\mathbf{F}-2/3\tilde{I}_1\mathbf{F}^{-T}\right) \tag{10}$$

$$\mathbf{P}_{fAB}^0=2\mathbf{F}\,\partial W_{fAB}/\partial\mathbf{C}=2\left(C_4/\alpha_4\right)\left\{\exp\left[\alpha_4\left(I_4-1\right)\right]-1\right\}\mathbf{F}\left(\mathbf{a}_0\otimes\mathbf{a}_0\right) \tag{11}$$

$$\mathbf{P}_{fT}^0=2\mathbf{F}\,\partial W_{fT}/\partial\mathbf{C}=2\left(C_6/\alpha_6\right)\left\{\exp\left[\alpha_6\left(I_6-1\right)\right]-1\right\}\mathbf{F}\left(\mathbf{b}_0\otimes\mathbf{b}_0\right) \tag{12}$$

According to the mechanics of visco-elastic materials, differential equations are introduced to specify the evolution of viscous variables:

$$\dot{\mathbf{q}}_m+\frac{1}{\tau_m}\mathbf{q}_m=\frac{\gamma_m}{\tau_m}\mathbf{P}_m^0 \tag{13}$$

$$\dot{\mathbf{q}}_{fAB}+\frac{1}{\tau_{fAB}}\mathbf{q}_{fAB}=\frac{\gamma_{fAB}}{\tau_{fAB}}\mathbf{P}_{fAB}^0 \tag{14}$$

$$\dot{\mathbf{q}}_{fT} + \frac{1}{\tau_{fT}} \mathbf{q}_{fT} = \frac{\gamma_{fT}}{\tau_{fT}} \mathbf{P}^0_{fT} \tag{15}$$

where $\tau_m, \tau_{fAB}, \tau_{fT}$ are relaxation times, as measures of time for the viscous processes development, $\gamma_m, \gamma_{fAB}, \gamma_{fT}$ are relative stiffness defining the stiffness contribution of viscous processes.

Identification of constitutive parameters

The identification of constitutive parameters was performed comparing model results and the average curves from cyclic tests on tissue specimens at different strain rates. The shape conformation of the experimental samples allows the assumption of an homogeneous distribution of stress and stretch fields within the central region of the specimen. Consequently, analytical models can be developed to interpret the experimental situations. The models define the trends of nominal stress with stretch along both apex-to-base and transverse directions. If directions 1, 2 and 3 are oriented respectively in apex-to-base, transverse and thickness directions in bladder, for a uniaxial loading condition, the deformation gradient can be assumed as a diagonal tensor with principal stretches λ_1, λ_2, λ_3. In detail, λ_1, λ_2 specify the imposed stretch conditions for uniaxial tests in apex-to-base or transverse direction, respectively, while λ_3 is the stretch in the thickness direction. Fibre orientations $\mathbf{a}_0$ and $\mathbf{b}_0$ can be evaluated as:

$$\mathbf{a}_0 = [1, 0, 0], \quad \mathbf{b}_0 = [0, 1, 0] \tag{16}$$

Accounting for the deformation gradient assumed and the orientation of fibres, the specific formulations of nominal stress components can be evaluated. In detail, the analytical model has to provide the stress component P_{11}^{mod} for an experimentally imposed stretch λ_1^{exp}, with regard to tests developed along the apex-to-base direction, and the stress component P_{22}^{mod}

for an experimentally imposed stretch λ_2^{exp}, with regard to tests along the transverse direction. With regard to the data from uniaxial tensile tests at disposal, the stretch along the loading direction is experimentally evaluated. Considering that the first Piola-Kirchhoff stress tensor depends on all the principal stretches and the stretch components that are not experimentally evaluated must be calculated by analytical methods, as reported by the following equations:

$$P_{jj}\left(\lambda_i,\lambda_j,\lambda_k\right)=0,\;\; P_{kk}\left(\lambda_i,\lambda_j,\lambda_k\right)=0 \tag{17}$$

The subscript i specifies the loading direction depending on the specific experimental situation, as apex-to-base or transverse directions. The stress components along the remaining directions j and k are null, because of the uniaxial configuration of experimental tests. Accounting for the experimental value of stretch component $\lambda_i^{\exp}$, the solution of the algebraic non-linear system, as reported in (17) leads to stretch components λ_j, λ_k, making it possible to evaluate the nominal stress component $P_{ii}\left(\lambda_i^{\exp},\lambda_j,\lambda_k\right)$ along the loading directions.

The procedure adopted for the definition of the constitutive parameters requires the minimization of the discrepancy between experimental and model results through a specific cost function. The cost function used (Natali et al., 2010) is reported in equation (18) where the weight of each data in the output is related with the ratio between the experimental data and model results:

$$\begin{aligned}\Omega(\boldsymbol{\omega}) = & \sqrt{\frac{1}{n^1}\sum_{z=1}^{n^1}\left(2-\frac{P_{11}^{\exp}{}_z}{P_{11}^{\text{mod}}{}_z\left(\boldsymbol{\omega},\lambda_1^{\exp}{}_z\right)}-\frac{P_{11}^{\text{mod}}{}_z\left(\boldsymbol{\omega},\lambda_1^{\exp}{}_z\right)}{P_{11}^{\exp}{}_z}\right)}+ \\ & +\sqrt{\frac{1}{n^2}\sum_{z=1}^{n^2}\left(2-\frac{P_{22}^{\exp}{}_z}{P_{22}^{\text{mod}}{}_z\left(\boldsymbol{\omega},\lambda_2^{\exp}{}_z\right)}-\frac{P_{22}^{\text{mod}}{}_z\left(\boldsymbol{\omega},\lambda_2^{\exp}{}_z\right)}{P_{22}^{\exp}{}_z}\right)}\end{aligned} \tag{18}$$

where $\boldsymbol{\omega}$ is the set of constitutive parameters, n^1 and n^2 the numbers of experimental data along apex-to-base and transverse directions, respectively, $\lambda_1^{\exp}{}_z$ or $\lambda_2^{\exp}{}_z$ the z^{th}

experimental input datum, ${P_{11}^{\exp}}_z$ or ${P_{22}^{\exp}}_z$ the z^{th} experimental output value, and ${P_{11}^{\text{mod}}}_z$ or ${P_{22}^{\text{mod}}}_z$ the z^{th} model output result corresponding to the constitutive parameters $\boldsymbol{\omega}$ and the experimental input ${\lambda_1^{\exp}}_z$ or ${\lambda_2^{\exp}}_z$. The function Ω is a measure of the overall difference between experimental and model results when constitutive parameters $\boldsymbol{\omega}$ are adopted. The problem involves the evaluation of the set of constitutive parameters $\boldsymbol{\omega}_{\text{opt}}$ that minimizes Ω.

RESULTS

Results from experimental tests on tissue samples are reported in Figure 2. In detail average curves are reported for the different experimental situations investigated, as loading-unloading steps along different directions and according to different strain rates. Transverse specimens show a greater stiffness that apex-to-base ones. The result agrees with histological conformation of the tissue, as predominant distribution of muscular fibers along circumferential direction (Bouhout et al., 2013; Korossis et a. 2009; Zanetti et al., 2012). The transverse response shows a greater influence of the strain rate on the stress-strain curve respect to the apex-to-base response, due to the different distribution of fibrous components along the different directions. High level strain rates are adopted to outline the variation of tissue response in loading-unloading phases and to identify short term response more appropriately.

The analysis of data from experimental investigations allowed to provide a visco-hyperelastic constitutive formulation, whose parameters have been identified by the inverse analyses of the mechanical tests. The optimal parameters are reported in Tables 2 and 3, with regard to hyperelastic and viscous contributions, respectively. According to the histological conformation of the tissue and the results from experimental activities, hyperelastic parameters C_4, α_4 which characterize the fibers stiffness along apex-to-base direction, assume smaller values than C_6, α_6 which characterize the fibers stiffness along transverse direction.

The capability of the model to interpret the mechanical behavior of bladder tissues is reported in Figures 3 and 4. With regard to the different loading conditions investigated, experimental data, as average trends and scatter bands evaluated per sample, and model curves are compared in Fig. 3a-e and Fig. 4a-e. Model results are proposed again in Fig. 3f and Fig. 4f. Results from the loading steps only are reported, to better show the influence of strain rate on the mechanical response. An additional analysis has been performed in order to check results affinity between the different pigs, demonstrating the marginal influence of the specific animal on variability of experimental data.

In order to further evaluate the capability of the model to interpret dissipative phenomena, the areas of hysteresis cycles are computed. Experimental and model results are compared in Figure 5.

Finally, the developed constitutive framework is applied to evaluate bladder tissue response under different loading conditions, as repetitive cyclic loading and stress relaxation. With regard to the former situation, model results for loading tests along apex-to-base and transverse directions are reported in Figure 6. The peak stress and the hysteresis area progressively decrease with the number of cycles up to stabilization.

DISCUSSION AND CONCLUSION

The constitutive analysis of bladder tissues is performed to provide a visco-hyperelastic framework that is capable to interpret the general features of bladder tissues mechanics. The analysis requires an integrated approach, accounting for the review of histological data to evaluate the tissues structural configuration, the design and development of experimental tests to provide the mechanical data, the constitutive model and to identify the associated parameters. The testing protocol included storing specimens at -20°C, as done also by other authors (Dahms et al. 1998Tissue). As illustrated in the following, results agree with finding of other researchers who simply stored the biological material at +4°C and tested it within 48 h (Van Mastrigt et al., 1981; Salinas et al., 1992; Nagatomi et al., 2004). Nevertheless, a systematic analysis of the effects of storage temperature on mechanical properties of the specific tissue is still lacking in literature, while experience confirms the poor effects in other soft tissues.

Tissue conformation suggests to perform mechanical tests along different loading directions. Marginal discrepancies are found in literature data along the transverse direction compared to the apex-to-base direction, probably due to the strain levels assumed, where collagen fibres elongation becomes the dominant phenomenon (Korossis et al., 2009). The dissipative behavior does not show a high level of anisotropy, and this result is in accordance with observations from other authors (Regnier et al., 1983; Salinas et al., 1992; Nagatomi et al., 2004; Chen et al., 2013). Accounting for the histological data at disposal and results from the developed mechanical tests, a constitutive formulation is provided in the framework of fibre-reinforced composite materials visco-hyperelasticity. Considering the histological data reported in the literature (Bouhout et al., 2013; Korossis et a. 2009) and results from the developed mechanical tests, the constitutive parameters are identified by the inverse analysis of the experimental tests.The capability of the proposed constitutive formulation to interpret the mechanics of bladder tissues is shown in Fig. 2, 3 and 4. From a qualitative point of view, model results well interpret the trends of the experimental data. From a quantitative point of view, model curves are well placed within the domains of the experimental results, and the calculated energy loss values fall within the variability of experimental data, and are generally very close to their average value. With specific regard to viscous phenomena, the identified parameters (Table 3) agree with results from other authors (Van Mastrigt et al., 1981; Salinas et al., 1992; Nagatomi et al., 2004).

The constitutive formulation also allowed to forecast tissue behaviour whenever the specimen undergoes consecutive cycles. According to both model and experimental results, the mechanical properties of the tissue change significantly. More likely, it shows that the employed loading rate in cyclic tests has not allowed full tissue recovery (Bischoff et al., 2004). Finally, according to the set up model, the stress relaxation behaviour is strongly dependent on strain rate: at lower strain rate, the tissue response is slower, reaching a smaller peak stress, and decaying with a longer time constant.

Analyses are developed to verify the capability of the constitutive model developed to interpret the mechanical response of the bladder tissue in physiological condition. Additional model results from stress relaxation conditions are reported in Figure 7. Stress relaxation phenomena are investigated assuming a 50% stretch condition which is reached according to different strain rates aiming at an interpretation of physiological condition.

Further investigations should be developed to improve the efficacy of results. Different loading conditions should be analyzed, as tensile tests along different directions to assess the assumption about anisotropic configuration and bi-axial tests to better evaluate the planar response. Nevertheless, the here proposed activities allows to quantitatively appreciate the typical features of bladder tissue mechanics, as direction dependence, non-linear elasticity and time-dependence. The experimental activities have been developed on animal model, because of the availability of samples and the similarity between pig and human bladder structures. Aiming at the characterization of human bladder tissue mechanics, the further step of the investigation will have to account for the development of experimental activities on human samples. The number of samples will be necessarily small. The qualitative trend of tissue mechanics will be identified by the results from the experimental activities on pig samples, while the quantitative behavior will be tuned by the results from activities on human tissue.

The proposed constitutive analysis provides a procedure that should be adopted to perform the mechanical characterization of the different tissues of the urinary tract, which is mandatory for the definition of numerical models of the biological structures. In this way it is posssible to investigate tissues response in healthy conditions and can be extended to degenerative conditions in the light of previous experience on damage models in soft tissue mechanics (Natali et al., 2003; Natali et al., 2008). Experience in surgical practice confirms the capability to provide a substitution following radical cystectomy (Abol-Enein et al., 2001; Kock et al., 1982; Hautmann et al., 1999; Pagano et al., 1990; Stein et al., 2004; Studer et al., 2006) by means of a specific technique that entails the use of substitute tissues that must guarantee the biomechanical performances, also in case of aged patients and considering potential local degenerative conditions. In fact, the present work must be considered as a preliminary step for the interpretation of biomechanical functionality and its correlation with surgical techniques. More in detail, the attention must be focused on mechanical actions induced on biological tissues during surgery and in the post-surgical configuration. It must be pointed out that computational methods allow the evaluation of structural data as the strain and stress fields, able to identify the tissue response. These data cannot be acquired by experimental techniques, with the same accuracy and richness of information, while they are mandatory for a reliable assessment of the applied mechanical actions.

Acknowledgment

This research received no specific grant from any funding agency in the public, commercial, or not-for-profit sectors.

Word Count: 3940

REFERENCES

Abol-Enein, H., Ghoneim, M.A.,2001. Functional results of orthotopic ileal neobladder with serous-lined extramural ureteral reimplantation: experience with 450 patients. Journal of Urology 165:1427–32.

Bischoff, E., Arruda, E.M., Grosh, K., 2004. A rheological network model for the continuum anisotropic and viscoelastic behavior of soft tissue. Biomechanics and Modeling in Mechanobiology 3:56–65.

Carniel, E.L., Fontanella, C.G., Polese, L., Merigliano, S., Natali, A.N.,2013. Mechanics of biological tissues and structures of the gastrointestinal region. Technology and health care 21:271-283.

Carniel, E.L., Gramigna, V., Fontanella, C.G., Stefanini, C., Natali, A.N., 2014. Constitutive formulations for the mechanical investigation of colonic tissues. Journal of Biomedical Materials Research Part A 1024A:1243-1254.

Chai, X., van Herk, M., Hulshof, M.C.C.M., Bel, A., 2012. A voxel-based finite element model fot the prediction of the bladder deformation. Medical Physics. 39:55 doi: 10.1118/1.3668060.

Chen, J., Drzewiecki, B.A., Meyyman, W.D., Pope, IV J.C., 2013. Murine bladder wall biomechanics following partial bladder obstruction. Journal of Biomechanics 46:2752-2755.

Dahms, S.E., Piechota, H.J., Dahiya, R., Lue, T.F., Tanagho, E.A., 1998. Composition and biomechanical properties of the bladder acellular matrix graft: comparative analysis in rat, pig and human. British Journal of Urology 82:411-419.

Fontanella, C.G., Matteoli, S., Carniel, E.L., Wilhjelm, J.E., Virga, A., Corvi, A., Natali, A.N., 2012. Investigation on the load-displacement curves of a human healthy heel pad: In vivo compression data compared to numerical results. Medical Engineering and Physic 34:1253-1259.

Fontanella, C.G., Forestiero, A., Carniel, E.L., Natali, A.N., 2013. Analysis of heel pad tissues mechanics at the heel strike in bare and shod conditions. Medical Engineering and Physic 35:441-447.

Forestiero, A., Carniel, E.L., Natali, A.N., 2014. Biomechanical behaviour of ankle ligaments: constitutive formulation and numerical modelling. Computer Methods in Biomechanics and Biomedical Engineering 17:395-404.

Irwin, D.E., Milson, I., Hunskaar, S., Reilly, K., Kopp, Z., Herschorn, S., Coyne, K., Kelleher, C., Hampel, C., Artibani, W., Abrams, P., 2006. Population-Based Survey of Urinary Incontinence, Overactive Bladder, and Other Lower Urinary Tract Symptoms in Five Countries: Results of the EPIC Study. European Urology 50(6): 1306-1315.

Hampel, C., Artibani, W., Espuna, P.M., Haab, F., Jackson, S., Romero, J., Gavart, S., Papanicolaou, S., 2004. Understanding the burden of stress urinary incontinence in Europe: a qualitative review of the literature. European Urology 46: 15–27.

Hautmann, R.E., de Petriconi, R., Gottfried, H.W., Kleinschmidt, K., Mattes, R., Paiss, T., 1999. The ileal neobladder: complications and functional results in 363 patients after 11 years of followup. Journal of Urology 161:422–7.

Kock, N.G., Nilson, A.E., Nilsson, L.O., Norlen, L.J., 1982. Philipson BM. Urinary diversion via a continent ileal reservoir: clinical results in 12 patients. Journal of Urology 128:469–75.

Korossis, S., Bolland, F., Southgate, J., Ingham, E., Fisher, J., 2009. Regional biomechanical and histological characterization of the passive porcine urinary bladder: implication for augmentation and tissue engineering strategies. Biomaterials 30:266–275.

Krywonos, J., Fenwick, J., Elkut, F., Jenkinson, I., Liu, Y.H., Brunt, J.N.H., Scott, A., Malik, Z., Eswar, C., Ren, X.J., 2010. MRI image-based FE modelling of the pelvis system and bladder filling. Computer Methods in Biomechanics and Biomedical Engineering 13:669-676.

Marino, G., Bignardi, C., 2002. Reconstruction, application and evaluation of a finite element method to study the pelvic floor. Preliminary resultsMinerva Urologica e Nefrologica 54:183-187.

Mavrilas, D., Sinouria, E.A., Vynios, D.H., Papageorgakopoulou, N. Dynamic mechanical characteristics of intact and structurally modified bovine pericardial tissues . Journal of Biomechanics 38: 761–768.

Nagatomi, J., Gloeckner, D.C., Chancellor, M.B., DeGroat, W.C., Sacks, M.S., 2004. Changes in the biaxial viscoelastic response of the urinary bladder following spinal cord injury. Annals of Biomedical Engineering 32:1409-1419.

Natali, A.N., Pavan, P.G., Carniel, E.L., Dorow, C., 2003. A transversally isotropic elastodamage constitutive model for the periodontal ligament. Computer Methods in Biomechanics and Biomedical Engineering 6: 329-336.

Natali, A.N., Pavan, P.G., Carniel, E.L., Dorow, C., 2004. Visco-elastic response of the periodontal ligament: an experimental-numerical approach. Connective Tissue Research 45:222–230.

Natali, A.N., Carniel, E.L., Pavan, P.G., Sander, F.G., Dorow, C., Geiger, M., 2008. A visco-hyperelastic-damage constitutive model for the analysis of the biomechanical response of the periodontal ligament. ASME Journal of Biomechanical Engineering 130(3): 031004.

Natali, A.N., Fontanella, C.G., Carniel, E.L., 2010. Constitutive formulation and analysis of heel pad tissues mechanics. Medical Engineeering and Physic 32:516-522.

Natali, A.N., Fontanella, C.G., Carniel, E.L., Miller-Young, J., 2011. Biomechanical behaviour of heel pad tissue. Experimental testing, constitutive formulation, and numerical modeling. Proceedings of the Institution of Mechanical Engineers, Part H 225:449-459.

Natali, A.N., Fontanella, C.G., Carniel, E.L., 2012. A numerical model for investigating the mechanics of calcaneal fat pad region. Journal of the Mechanical Behavior of Biomedical Materials 5:216-223.

Pagano, F., Artibani, W., Ligato, P., Piazza, R., Garbeglio, A., Passerini, G., 1990. Vescica ileale Padovana: a technique for total bladder replacement. . European Urology 17:149–54.

Pal, S.J., Muthu, P., Muhuri, A.D., 2013. 3D modeling of lower urinary tract to analyze lower urinary tract constriction. Journal of Mechanical and Civil Engineering 31-38.

Pel, J.J., van Mastrigt, R., 2007. Development of a CFD urethral model to study flow-generated vortices under different conditions of prostatic obstruction. Physiological Measurement 28:13-23.

Regnier, C.H., Kolsky, H., Richardson, P.D., Ghoniem, G.M., Susset, J.G., 1983. The elastic behavior of the urinary bladder for large deformations. Journal of Biomechanics 16:915-922.

Sacco, E., Praier-Galetti, T., Pinto, F., Francalanza, S., Betto, G., Pagano, F., Artibani, W., 2006. Urinary incontinence after radical prostatectomy: incidence by definition, risk factors and temporal trend in a large series with a long-term follow-up. BJU International 97(6): 1234-1241.

Salinas, J., Virseda, M., Fuente, M.P., Mellado, F., Uson, A.C., 1992. A study on the viscoelastic properties of the urinary bladder in dogs. Urologia Internationalis 49:185-190.

Silver, F.H., Seehra, G.P., Freeman, J.W., DeVore, D., 2002. Viscoelastic properties of young and old human dermis: A proposed molecular mechanism for elastic energy storage in collagen and elastin. Journal of Applied Polymer Science 86:1978-1985.

Stein, J.P., Dunn, M.D., Quek, M.L., Miranda, G., Skinner, D.G., 2004. The orthotopic T pouch ileal neobladder: experience with 209 patients. Journal of Urology 172:584–7.

Studer, U.E., Burkhard, F.C., Schumacher, M., 2006. Twenty years expe- rience with an ileal orthotopic low pressure bladder substitute— lessons to be learned. Journal of Urology 176:161–6.

Van mastrigt, R., Nagtegaal, J.C., 1981. Dependence of the viscoelastic response of the urinary bladder wall on strain rate. Medical & Biological Engineering & Computing 19: 291-296.

Vlastelica, I., Veljkovic, D., Rankovic, V., Stojanovic, B., Rosic, M., Kojic, M., 2007. Modeling of urinary bladder deformation within passive and active regimes. Journal of the Serbia Society for Computational Mechanics 1:129-134.

Weiss, J.A., Maker, B.N., Govindjee, S., 1996. Finite element implementation of incompressible, transversely isotropic hyperelasticity. Computational Methods in Applied Mathematics 135:107–128.

Zanetti, E.M., Perrini, M., Bignardi, C., Audenino, A.L., 2012. Bladder tissue passive response to monotonic and cyclic loading. Biorheology 49:49-63.

Bladder tissue biomechanical behavior: experimental tests and constitutive formulation

FIGURE AND TABLE LEGENDS

Table 1. Number of specimen and their average width and thickness.

Table 2. Set of hyperelastic constitutive parameters.

Table 3. Set of viscous constitutive parameters.

Figure 1. Bladder dissection and region definition: (a) bladder in the anterior-posterior view with indication of the track of dissection plane; (b) cut-opened bladder showing the apex, the lateral and the base region of the bladder.

Figure 2. Average experimental data along apex-to-base (AB) and transverse (T) direction: (a) strain rate 10 %/s, (b) strain rate 50 %/s, (c) strain rate 100 %/s, (d) strain rate 200 %/s, (e) strain rate 500 %/s.

Figure 3. Comparison of the tensile stress-strain along apex-to-base (AB) direction of experimental data (average ± standard deviation) and analytical results: (a) strain rate 10 %/s, (b) strain rate 50 %/s, (c) strain rate 100 %/s, (d) strain rate 200 %/s, (e) strain rate 500 %/s. (f) Analytical results for the rising branch of loading cycles, at different strain rates.

Figure 4. Comparison of the tensile stress-strain along transverse (T) direction of experimental data (average ± standard deviation) and analytical results: (a) strain rate 10 %/s, (b) strain rate 50 %/s, (c) strain rate 100 %/s, (d) strain rate 200 %/s, (e) strain rate 500 %/s. (f) Analytical results for the rising branch of loading cycles, at different strain rates.

Figure 5. Strain energy loss at different rates: comparison between experimental (average ± standard deviation) and analytical data, for (a) apex-to-base and (b) transverse directions.

Figure 6. Stress strain cycles, as predicted by the model, at strain rate 200%/s, for (a) apex-to-base and (b) transverse directions.

Figure 7. Stress relaxation curves predicted by the constitutive model, at different rates, for (a) apex-to-base and (b) transverse directions.

Figure 1
Click here to download high resolution image

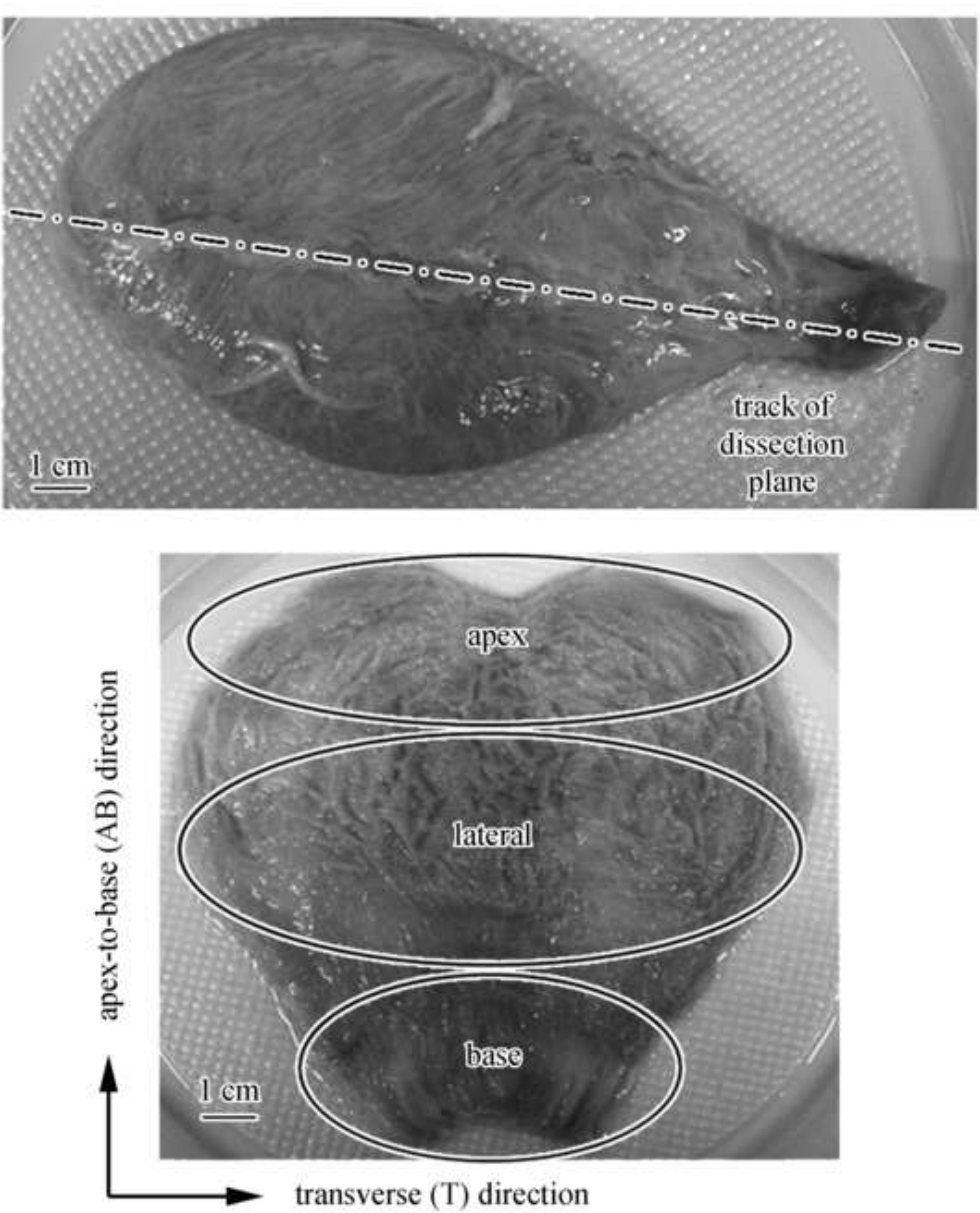

Figure 2
Click here to download high resolution image

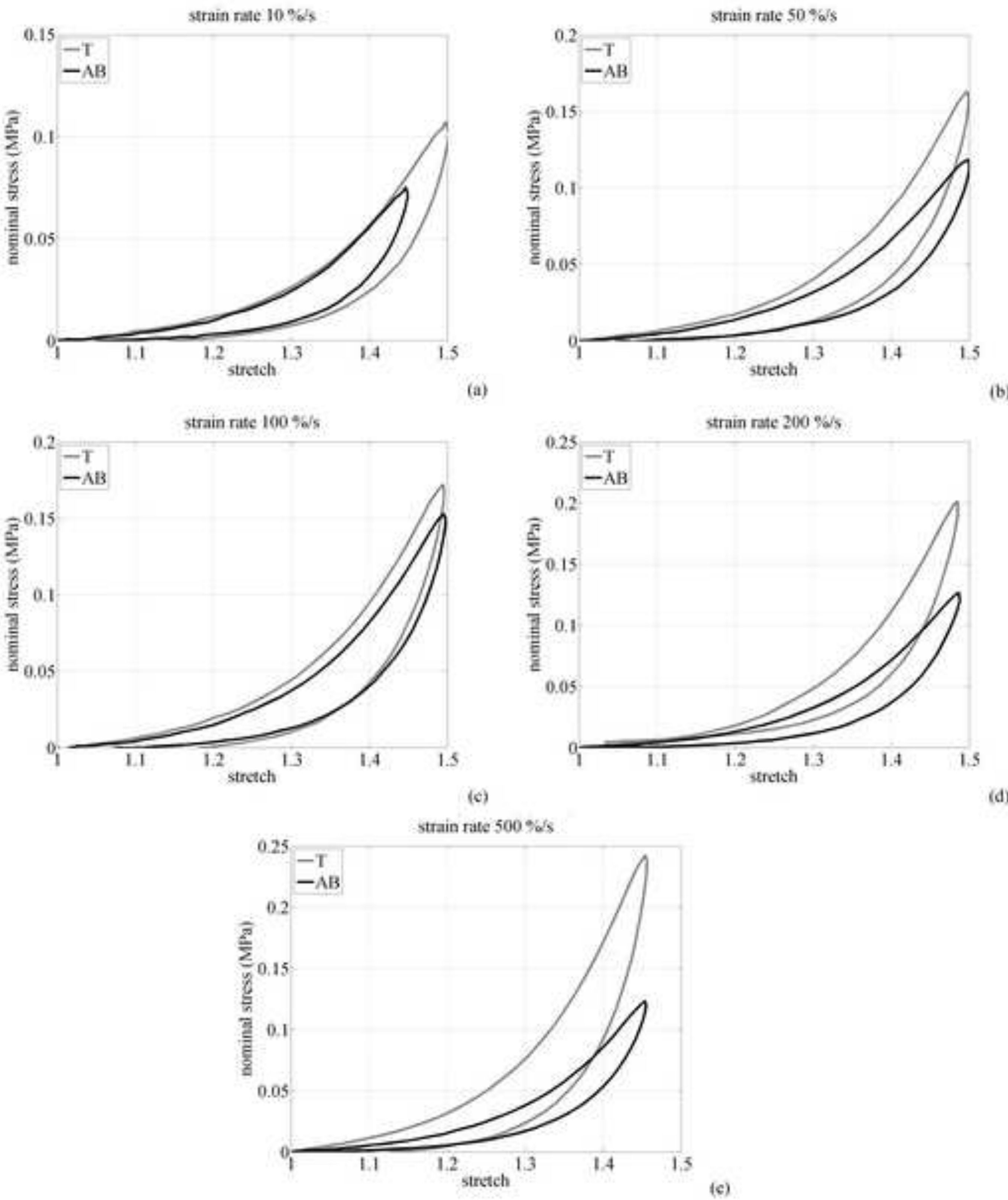

Figure 3
Click here to download high resolution image

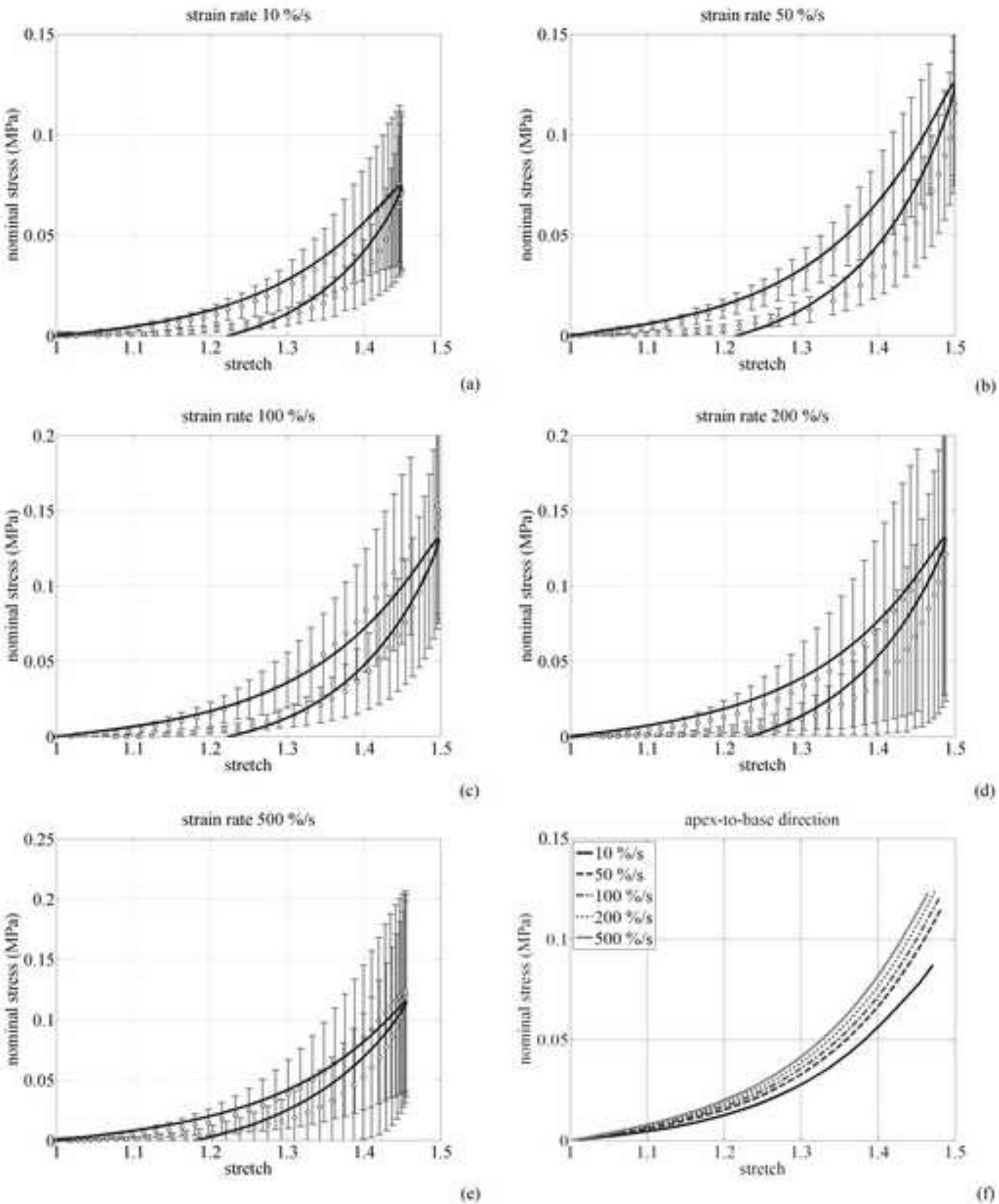

Figure 4
Click here to download high resolution image

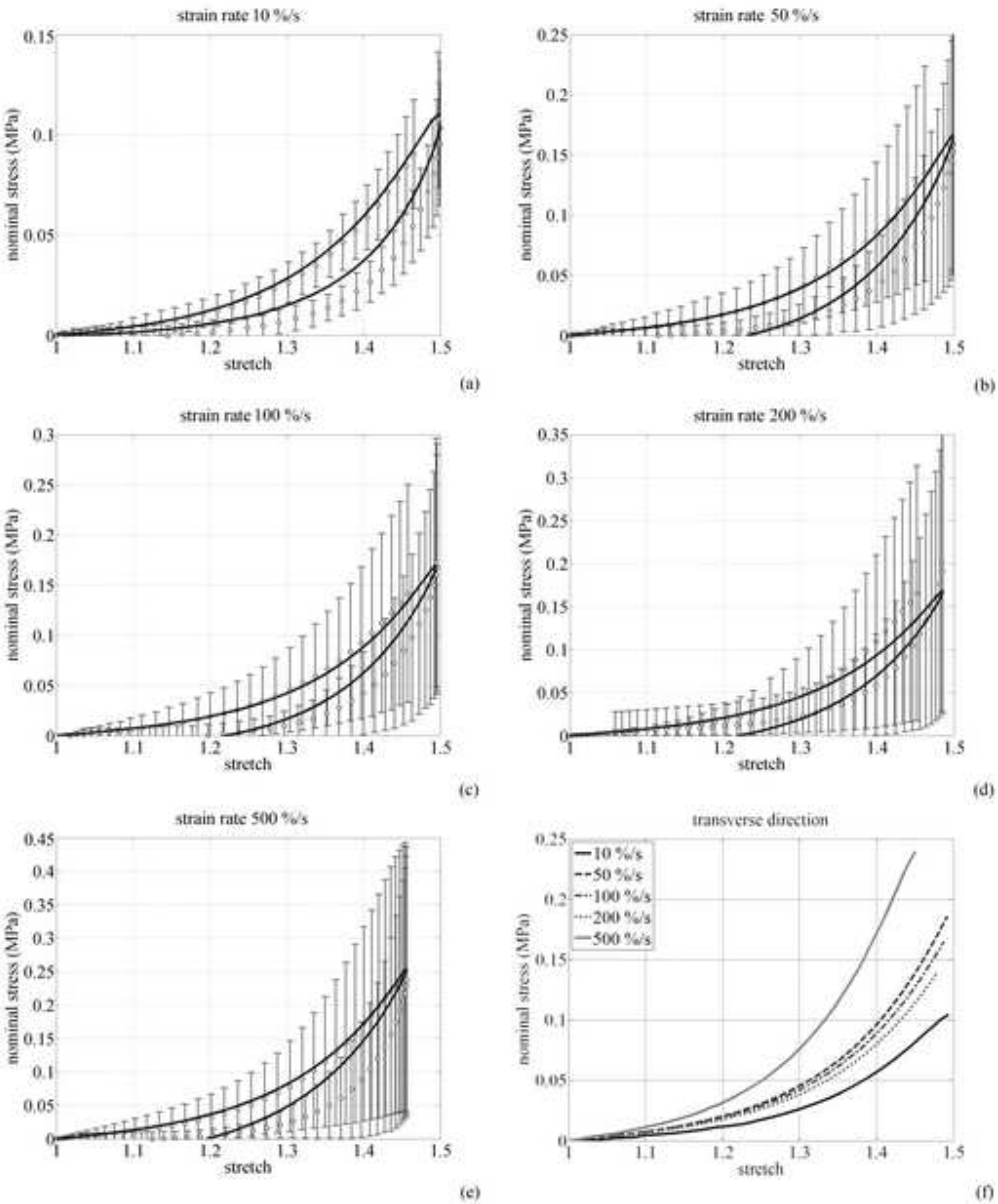

Figure 5

Click here to download high resolution image

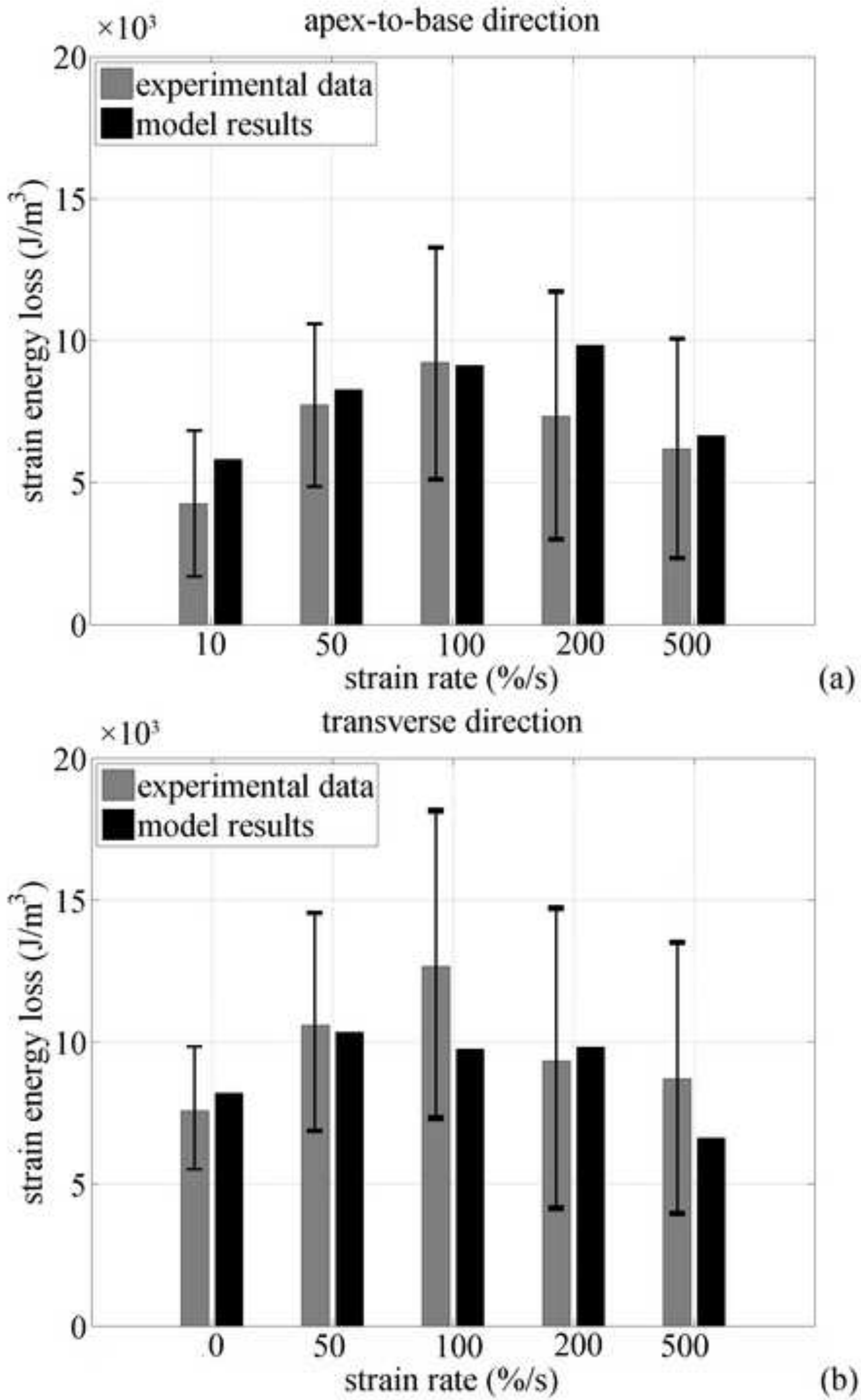

Figure 6
Click here to download high resolution image

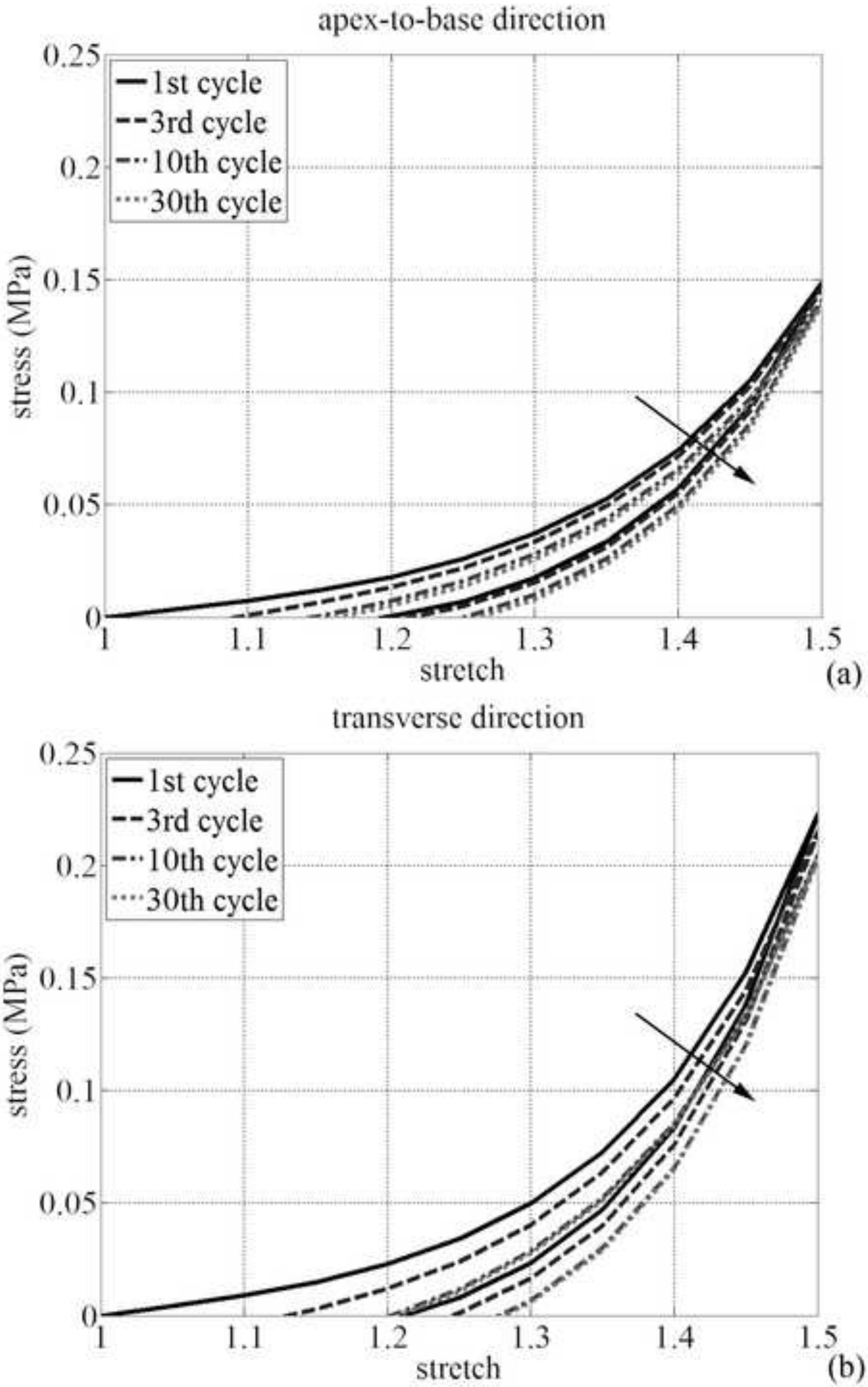

Figure 7
Click here to download high resolution image

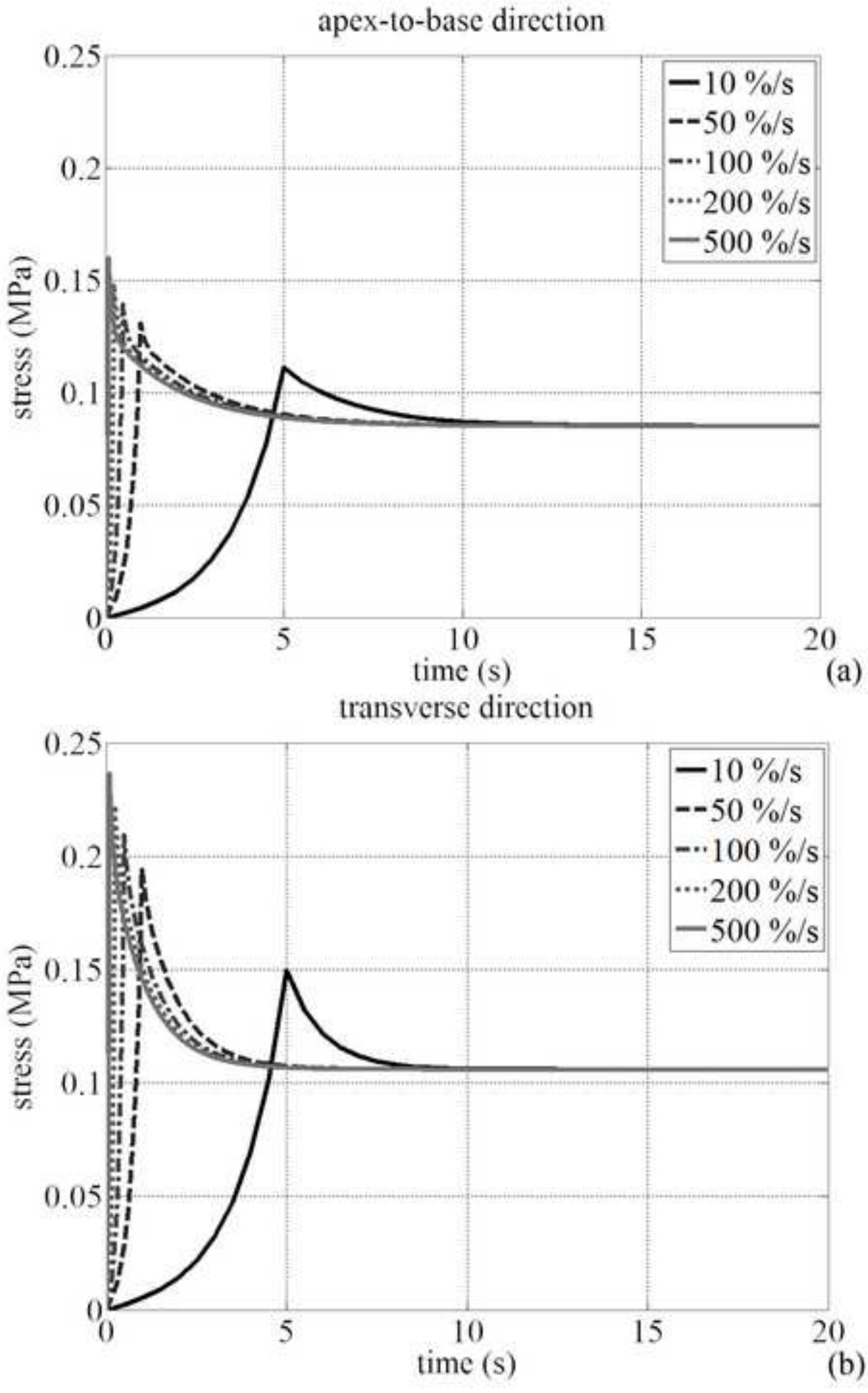

Table

TABLES

	No. of specimen	width mean ± standard deviation (mm)	thickness mean ± standard deviation (mm)
apex-to-base direction	9	4.95±0.56	4.37±1.00
transverse direction	16	4.49±0.78	3.77±1.03

Table 1

C_1 (MPa)	α_1	C_4 (MPa)	α_4	C_6 (MPa)	α_6
$5.96 \cdot 10^{-4}$	$2.20 \cdot 10^{0}$	$4.60 \cdot 10^{-3}$	$2.04 \cdot 10^{0}$	$4.80 \cdot 10^{-3}$	$2.25 \cdot 10^{0}$

Table 2

	γ	τ *(s)*
matrix viscous process (*m*)	$9.37 \cdot 10^{-1}$	$8.50 \cdot 10^{-2}$
apex-to-base viscous process (*fAB*)	$3.50 \cdot 10^{-1}$	$2.32 \cdot 10^{+0}$
transversal viscous process (*fT*)	$4.12 \cdot 10^{-1}$	$2.01 \cdot 10^{+0}$

Table 3